

Development of new cements environmentally friendly

Diana Margarida Câmara Santos

Extended Abstract

Materials' Engineering

Supervisor(s): Prof. Dr. Rogério Anacleto Cordeiro Colaço

Eng^o. Rodrigo Manuel Lino Santos

Examination Committee

Chairperson: Prof^a. Dr^a. Maria de Fátima Reis Vaz

Supervisor: Eng^o. Rodrigo Manuel Lino Santos

Members of the Committee: Prof. Dr. Ricardo Manuel Simões Bayão Horta

March 2015

Abstract

The main challenge of the cement industry is the reduction of CO₂ emissions associated to cement production. The alternative of the reduction of limestone (CaCO₃) incorporation in the raw-material was studied in this work. Clinkers with C/S ratio equal to 1,1 and 1,25 in the domain of wollastonite and rankinite whose hydraulic reactivity is extremely reduced or inexistent as reported in literature were produced. Pastes of the same clinkers were produced with the aim of determining the compression strength after 28 days and to relate with the structure properties of calcium silicate hydrate gel (C-S-H) produced by hydration. A comparative analysis with an alitic clinker typical of Portland cement was simultaneously performed.

Keywords: CO₂, clinker, hydration, calcium silicate hydrate (C-S-H)

1. Introduction

The poorly crystalline or amorphous calcium silicate hydrate gel (C-S-H) constitutes about 40-50% of the hydration products in hardened Portland cement paste and is the main responsible for some of its principal properties such as strength and durability. The C-S-H's molecular structure has been reported from comparisons with crystalline calcium silicate hydrates: 1,4-nm tobermorite and jennite are considered the most appropriate models [1, 2].

C-S-H gel has a variable stoichiometry with the calcium to silicon ratio (C/S) which varies in wide range from about 0,8 to 2 and with an average value of 1,7 for the conventional hydrated Portland cement [3]. However, the Ca/Si ratio of 1,4-nm tobermorite is 0,83 [1]. The Ca/Si ratio can be raised above 0,83 by the progressive random elimination of the bridging tetrahedron from the silicate chains creating SiO₂ vacancies and increasing the disorder of the structure. This mechanism is the principal characteristic in many other tobermorite-based models for C-S-H [4]. There is a consensus that the structure of C-S-H is composed essentially by tobermorite-like structure over the whole C/S ratio range [3].

C/S ratio is a measure of point defects (vacancies) in the silicate chain [5]. Removing silica tetrahedra from the tobermorite's structure with the aim of increasing C/S ratio reduces the short-range order [2, 5]. Thus, it is possible to observe a progression from a well ordered lamellar structure at C/S equal to 1,1 to a disordered structure at C/S equal to 1,8. The degree of polymerization of silica tetrahedra in C-S-H is denoted by the mean chain length (MCL) [5]. The degree of polymerization in C-S-H decreases nonlinearly with C/S ratio. Synthetic C-S-H with C/S 1 to 1,1 demonstrates on average 31% higher mechanical resistance comparatively to C-S-H with C/S equal to 1,7 produced by Portland cement hydration [5].

2. Experimental

2.1. Materials and processing conditions

In the present work, the clinkers with C/S ratio equal to 1,1 and 1,25 were obtained by a production cycle with the aim of forming a dendritic morphology of the crystalline phase during solidification. The high solidification speed responsible for the formation of dendrites, origins the

formation of amorphous structures typical of vitreous systems. In the $\text{CaO} \cdot \text{SiO}_2$ system, the amorphous structures at room temperature are unstable by nature. Thus, the hydraulic reactivity is expected to increase. The production cycle is presented in Figure 1 and consists of the follows steps:

- I. Heating at a rate $R_1 = 25^\circ\text{C}/\text{min}$ to temperature T_1 ;
- II. T_1 was maintained constant for $t_1 = 60$ min;
- III. Cooling at a rate $R_2 = 40^\circ\text{C}/\text{min}$ to temperature T_2 ;
- IV. T_2 was maintained constant for $t_2 = 1$ min;
- V. Cooling to room temperature naturally in air.

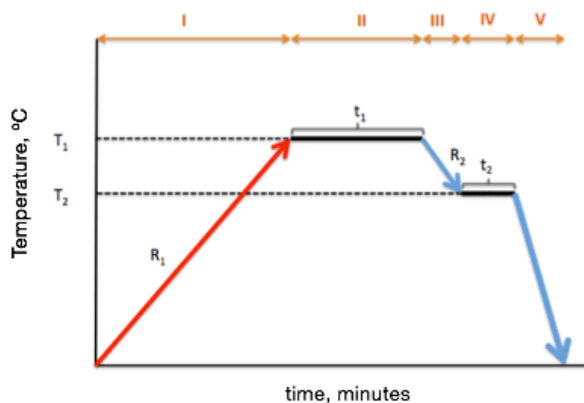


Tabela 1. Designation temperature cycle.

Designation temperature cycle	T_1 ($^\circ\text{C}$)	T_2 ($^\circ\text{C}$)
A	1500	1400
B	1450	1350
C	1400	1300
D	1350	1250
E	1300	1200

Figure 1. Schematic representation indicating the temperature cycle for the production of the clinkers.

The pastes were produced considering a water/clinker ratio of 0,375. Parallelepiped shape paste samples were produced with dimensions of $20 \times 20 \times 40 \text{ mm}^3$. The cure was achieved in a chamber at relative humidity of 90% and a temperature of 20°C .

2.2. Characterization methods

Compression strength determination was performed in an Ibertest Autotest 400/10 equipment.

Samples microstructures were observed by optical microscopy Olympus BX 60 with a CLEMEX camera.

Diffraction patterns of powder samples were collected in a PANalytical X'Pert Pro diffractometer in $\theta/2\theta$ configuration employing $\text{CuK}\alpha$ radiation ($\lambda = 1,54059 \text{ \AA}$). The samples were scanned between 5 to 70° (2θ) with a X'Celerator RTMS (Real Time Multiple Strip) detector. The X-ray tube worked at 45 kV and 40 mA .

ATR-FTIR analysis was performed using a Bruker Alpha Platinum-ATR spectrometer. The spectra were collected in the range from 400 to 4000 cm^{-1} , with 24 accumulations and a 4 cm^{-1} resolution.

Solid-state NMR analysis was performed using a TecMag/Bruker 300 "wide bore" instrument equipped with a 7 mm solid-state probe operating $59,6 \text{ MHz}$ for ^{29}Si . The spectra were collected under magic angle spinning (MAS) with a rate of about 3 KHz ; for the single (40° flip) pulse ^{29}Si NMR experiments a pulse length of $2 \mu\text{s}$ was used with a delay time of 10s .

3. Results and discussion

3.1. Optical Microscopy

Figure 2 shows optical microscopy images of the clinker samples produced. Samples 1.1_7.0_C and 1.25_AI1.7_A are completely amorphous.

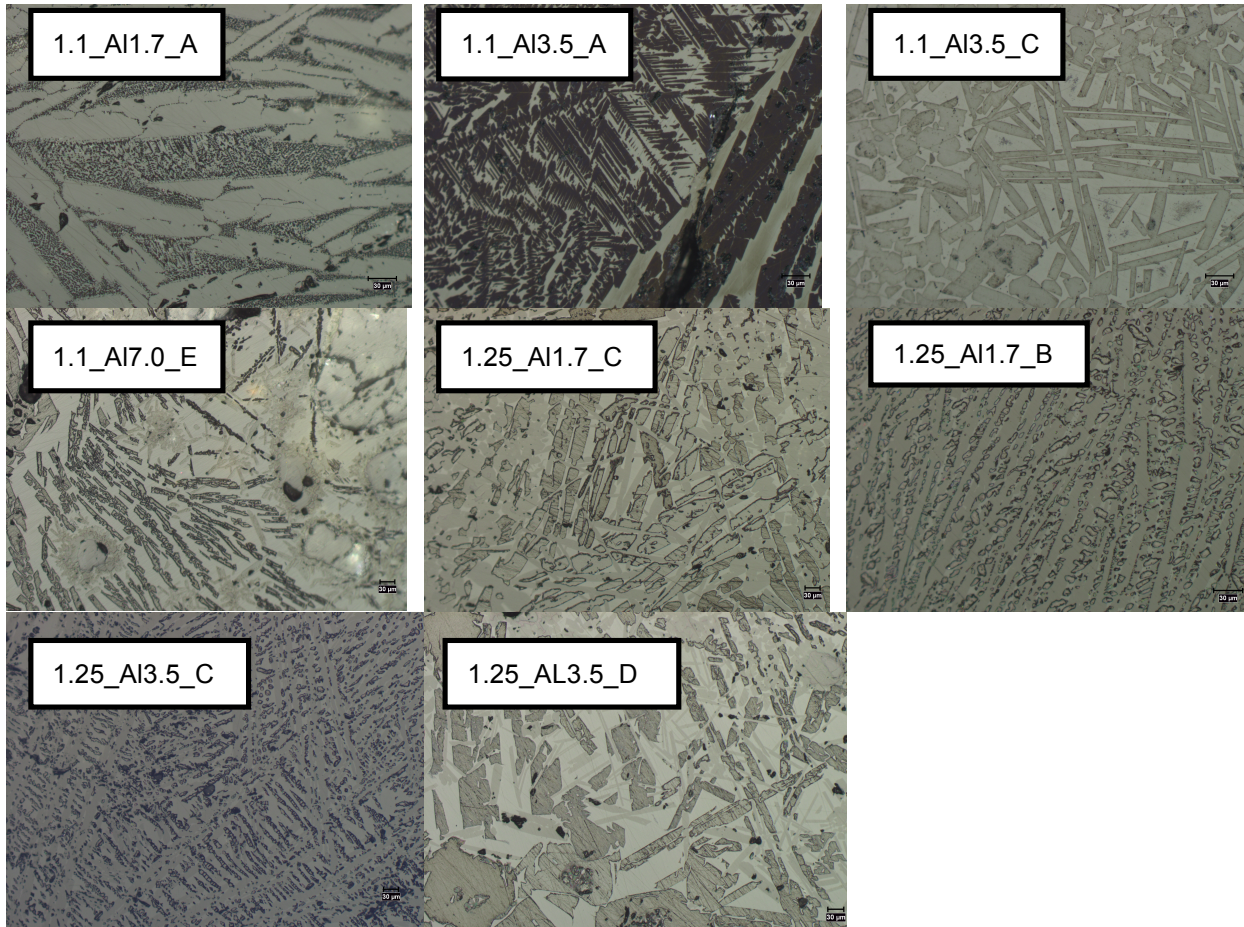


Figure 2. Microstructures of the clinkers produced.

3.2. Compression tests

The results of the compression test performed are present in Table 1. The sample 1.25_AI1.7_A showed the most interesting value of compression strength (18,7 MPa).

Table 1. Results of compression tests obtained for all samples studied in the present work.

Sample	Compression resistance 28 days (MPa)
Alitic	69,9
1.1_AI1.7_C	6,3
1.1_AI1.7_A	6,4
1.1_AI3.5_A	1,6
1.1_AI3.5_C	1,2
1.1_AI7.0_C	0,5
1.1_AI7.0_E	4,1
1.25_AI1.7_C	3,4
1.25_AI1.7_A	18,7
1.25_AI1.7_B	4
1.25_AI3.5_C	6,2
1.25_AI3.5_D	6,2

3.3. XRD/Rietveld

The most interesting result was obtained for sample 1.25_A11.7_A showed in Figure 3. Diffractogram of 1.25_A11.7_A clinker hydrated after 28 days showed a large diffraction band in the range of 26° e 34° indicating the amorphous nature of structure and peaks characteristics of crystalline tobermorite, by the presence of the phase 0.9nm-tobermorite (9° and 49,9°) and clinotobermorite (11° and 29,6°) (Rietveld analysis (Table 2) revealed 6,8% 0.9nm-tobermorite and 5,9% clinotobermorite).

It is possible to observe the absence of formation of portlandite during hydration in this clinker by the absence of its characteristic diffraction peak at 18°.

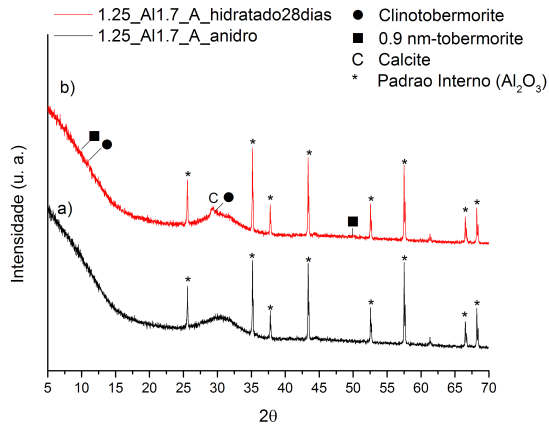


Table 2. Rietveld analysis 1.25_A11.7_A clinker.

		1.25_A11.7_A	
		Anhydrous	Paste 28 days
Rietveld wt%	Amorphous	100	84,5
	Calcite	-	2,8
	0.9nm-tobermorite	-	6,8
	Clinotobermorite	-	5,9

Figure 3. X-ray diffractogram of 1.25_A11.7_A clinker anhydrous (a) and hydrated 28 days (b).

3.4. Fourier Transform Infrared Spectroscopy

The ATR-FTIR spectra obtained for anhydrous alitic clinker (Figure 4) shows bands associated with alite at 910 cm⁻¹, 515 cm⁻¹ and 440 cm⁻¹ [6, 7] and a shoulder attributed to belite at 840 cm⁻¹ [8]. The band at 1132 cm⁻¹ is related to SO₃ [9]. The band present at 3640 cm⁻¹ is assigned to O-H stretching of portlandite (Ca(OH)₂) [6, 8]. The wide bands at 1488 cm⁻¹ and 1418 cm⁻¹ are attributed to C-O asymmetric stretching vibration of CO₃ group and the peak at 875 cm⁻¹ is assigned to bending out-of-plane vibration of CO₃ group [6, 8]. The main characteristic of hydrated alitic clinker spectra (Figure 4) is the decrease in intensity of the band at 910 cm⁻¹ and its displacement to 955 cm⁻¹, as well as the disappearance of the band 515 cm⁻¹ and the increase in intensity of 440 cm⁻¹, which indicates the calcium silicate polymerization and the formation of calcium silicate hydrate gel C-S-H [6, 8]. The band at 955 cm⁻¹ is related to the presence of Si-O bond asymmetric vibration of C-S-H. The band at 440 cm⁻¹ is assigned to Si-O bonding Si-O typical of tobermorite-like structures [6].

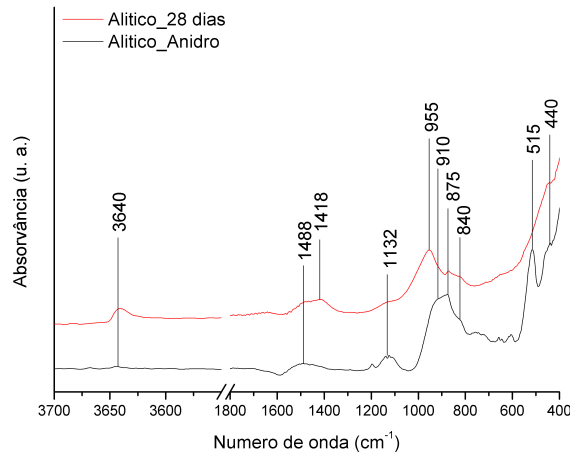


Figure 4. ATR-FTIR spectra of the anhydrous and hydrated after 28 days alitic clinker.

The bands at 1092 cm^{-1} , 1072 cm^{-1} , 985 cm^{-1} , 938 cm^{-1} , 916 cm^{-1} , 715 cm^{-1} , 563 cm^{-1} e 422 cm^{-1} are attributed to pseudowollastonite ($\alpha\text{-CaSiO}_3$) [10-12]. Peaks at 851 cm^{-1} , 656 cm^{-1} and 534 cm^{-1} are associated with rankinite (CaSi_2O_7). In particular, samples 1.25_AI1.7_B, 1.25_AI3.5_C showed peaks at 917 cm^{-1} , 510 cm^{-1} and a shoulder at 843 cm^{-1} associated with belite.

Comparing Figure 4 with Figure 5 and Figure 6 it is possible to observe that in the latter, with an exception to sample 1.25_AI1.7_A, displacement for higher wavenumbers of vibration bands is not observed. These results suggest that only the sample 1.25_AI1.7_A showed the formation of C-S-H gel because during hydration the intensity of band 937 cm^{-1} decreases and displaces to higher wavenumbers (958 cm^{-1}); this behavior together with the displacement of band from 485 cm^{-1} to 449 cm^{-1} , indicate the polymerization of SiO_4 tetrahedra and the formation of C-S-H, like the behaviour observed in ATR-FTIR spectra of the alitic clinker.

It is possible to observe the absence of formation of portlandite (Ca(OH)_2) during hydration in clinkers with ratio C/S 1,1 and 1,25 by the absence of its characteristic vibration band at 3640 cm^{-1} .

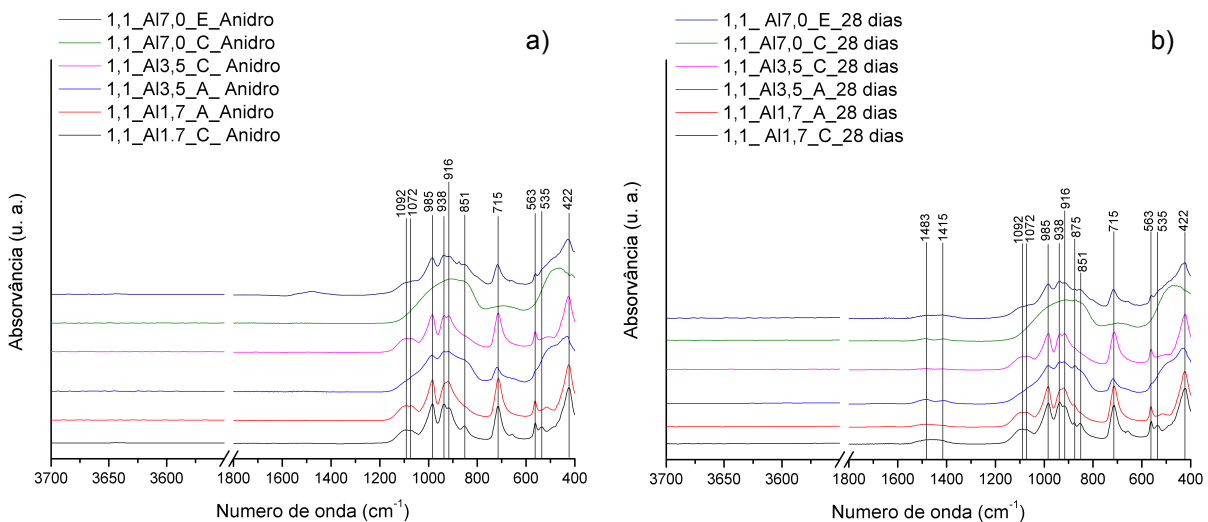


Figure 5. ATR- FTIR spectra of the anhydrous (a) and hydrated after 28 days (b) clinkers with ratio C/S 1.1.

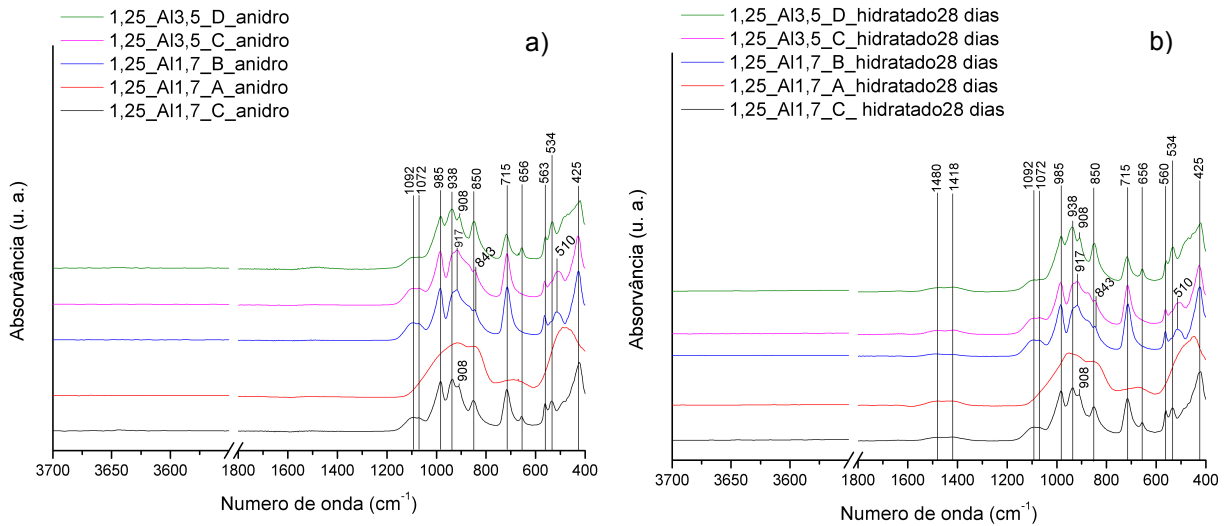


Figure 6. ATR-FTIR spectra of the anhydrous (a) and hydrated after 28 days (b) clinkers with ratio C/S 1.25.

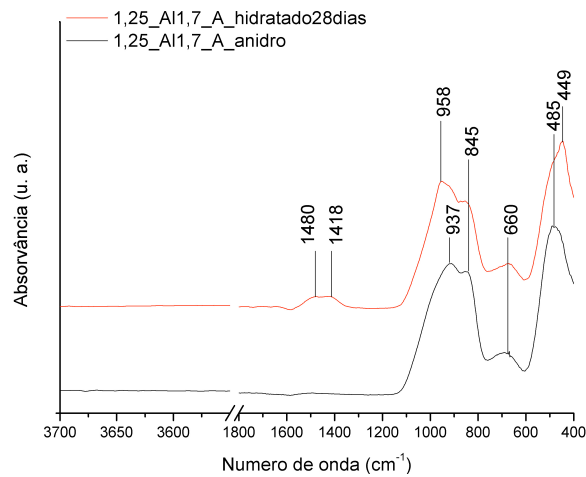


Figure 7. ATR-FTIR spectra of the anhydrous and hydrated after 28 days clinker 1.25_AI1.7_A.

3.5. ^{29}Si MAS-NMR Spectroscopy

Figure 8a) shows the ^{29}Si MAS-NMR spectra obtained for the anhydrous alitic clinker. The large band in the range -66 ppm to -74 ppm indicated that anhydrous calcium silicates, C_3S and $\beta\text{-C}_2\text{S}$, contain only Q^0 species. Figure 8b) shows the ^{29}Si MAS-NMR spectra obtained for the hydrated after 28 days alitic clinker whose it is possible to observe a decrease in intensity of band associated with anhydrous calcium silicates, with formation of Q^1 species at approximately -79,2 ppm and Q^2 species at approximately -84,2 ppm associated with C-S-H produced [2, 6, 13]. However, the most intense peak comes from Q^1 species so the majority of silica tetrahedra in C-S-H are organized in dimers [3]. The peak at -82 ppm is assigned to $\text{Q}^2(1\text{Al})$ [9].

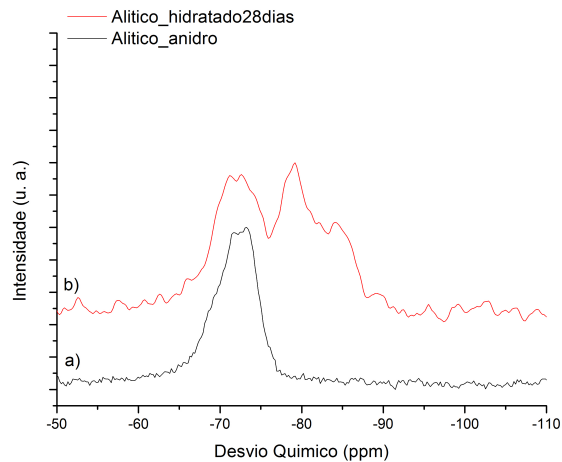


Figure 8. ^{29}Si MAS-NMR spectra of the anhydrous (a) and hydrated after 28 days (b) alitic clinker.

^{29}Si MAS-NMR spectra of 1.1_AI1.7_C and 1.25_AI3.5_D samples, Figure 9A and Figure 9E, respectively, shows resonance peaks at -74,5 ppm and -75,9 ppm assigned to Q^1 species of rankinite [14], peak at -83,5 ppm attributed to Q^2 species of pseudowollastonite [14]. Figure 9B presents the spectra obtained for 1.1_AI1.7_A sample whose it is possible to observe a peak at -83,5 ppm attributed to pseudowollastonite. ^{29}Si MAS-NMR spectra of 1.1_AI7.0_C sample, in Figure 9C, show a large band centered at approximately -74,5 ppm as a consequence of the amorphous structure of the sample. ^{29}Si MAS-NMR spectra of 1.25_AI1.7_A sample, in Figure 9D, show a peak at -71,3 ppm associated with Q^0 species of $\beta\text{-C}_2\text{S}$ [9] and a peak at -83,5 ppm attributed to Q^2 species of pseudowollastonite. Figure 9F presents a comparison of ^{29}Si MAS-NMR of 1.25_AI1.7_A clinker anhydrous and hydrated after 28 days. It is possible to observe the displacement of peak at ≈ -75 ppm to more negative chemical shifts, $\approx -78,6$ ppm, indicates increase in the polymerization degree of silicate chains after hydration and formation of Q^1 species of C-S-H. It is also possible to observe the formation of a peak at ≈ -85 ppm indicating the formation of Q^2 species of C-S-H. Therefore, there is an increase in the polymerization degree of silicate chains after hydration, indicating the formation of C-S-H produced by hydration of amorphous phase.

Comparing the results of ^{29}Si MAS-NMR obtained for clinkers with ratio C/S 1.1 and 1.25 with results obtained for the alitic clinker, it is possible to verify that the sample 1.25_AI1.7_A is the only one that shows the formation of C-S-H, justifying the superior value of compression resistance comparatively with the remaining samples with ratio C/S 1.1 and 1.25.

Deconvolution of ^{29}Si MAS-NMR spectrum obtained for 1.25_AI1.7_A clinker hydrated after 28 days makes possible to verify that, in C-S-H produced, silicate tetrahedras are mainly organized in Q^2 species and therefore the silicate chains are more polymerized than C-S-H produced by hydration of alitic clinker that is mainly dimeric.

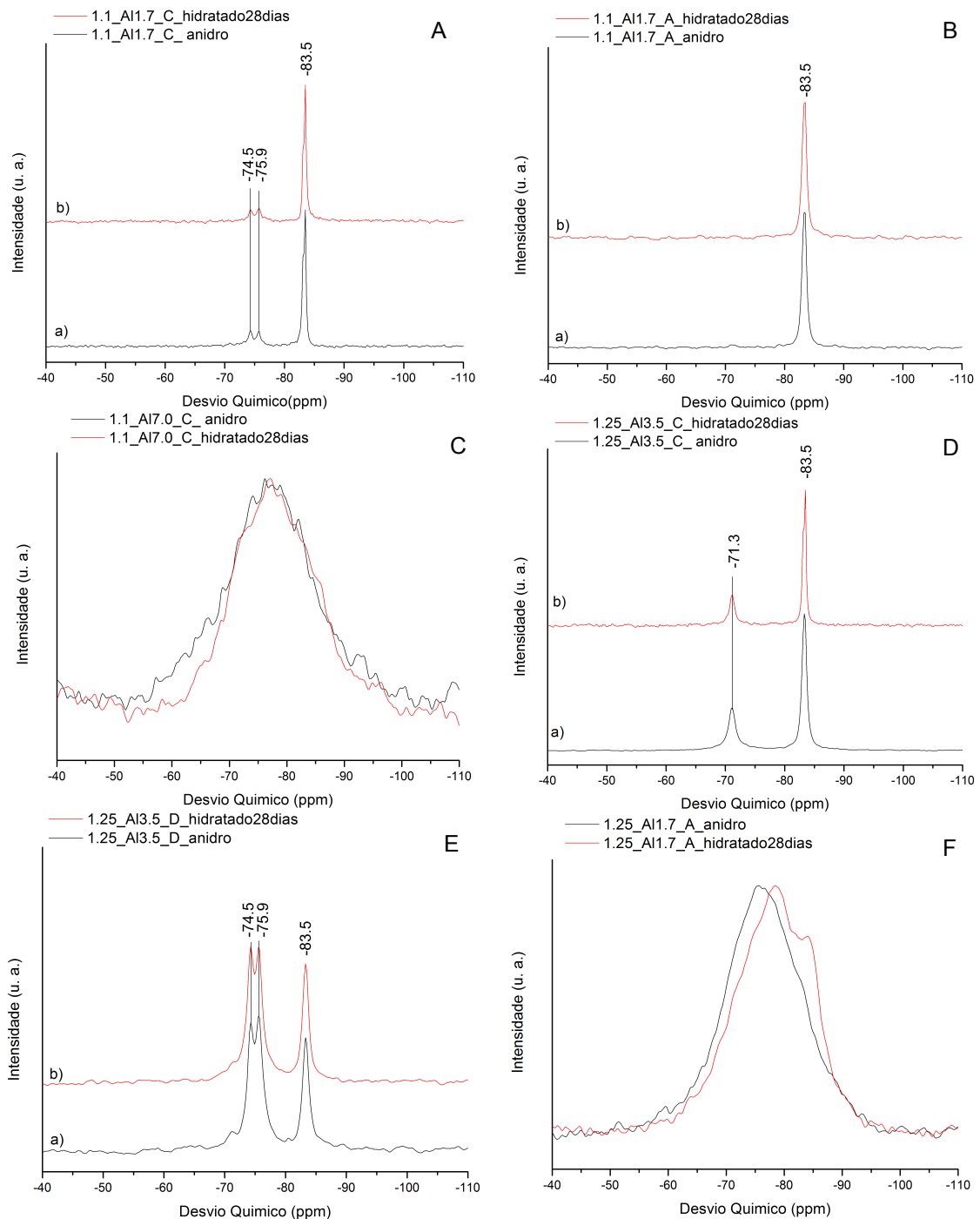


Figure 9. ^{29}Si MAS-NMR spectra of the anhydrous (a) and hydrated after 28 days (b) clinkers with ratio C/S 1.1 and 1.25.

4. Conclusion

The sample 1.25_A1.7_A, with a completely amorphous structure, showed the most promising results compared to the remaining samples with C/S ratio equal to 1.1 and 1.25. The paste of a clinker 1.25_A1.7_A showed a compression strength after 28 days equal to 18,7 MPa. The XRD/Rietveld analysis of the sample 1.25_A1.7_A hydrated after 28 days showed diffraction peaks characteristic of crystalline tobermorite. The ATR-FTIR spectrum of the sample 1.25_A1.7_A hydrated after 28 days presented the development of the bands related to the presence of C-S-H at $\approx 958\text{ cm}^{-1}$ and $\approx 449\text{ cm}^{-1}$. The ^{29}Si MAS-NMR analysis revealed an increase in the degree of silicate chains polymerization,

indicating the formation of C-S-H. It was demonstrated that C-S-H formed by hydration of clinker 1.25_A1.7_A has a higher polymerization degree comparatively with C-S-H formed by hydration of the alitic clinker. According to the results obtained with this work, it can be concluded that the development of clinker with ratio C/S 1.25 with promising hydraulic properties and able to reduce the CO₂ emission is possible.

References

1. Chen, J.J., et al., *Solubility and structure of calcium silicate hydrate*. Cement and Concrete Research, 2004. **34**(9): p. 1499-1519.
2. Taylor, H.F.W., *Cement Chemistry*. 1997, San Diego: Academic Press.
3. Kovačević, G., et al., *Atomistic modeling of crystal structure of Ca_{1.67}SiH_x*. Cement and Concrete Research, 2015. **67**(0): p. 197-203.
4. Richardson, I.G., *The calcium silicate hydrates*. Cement and Concrete Research, 2008. **38**(2): p. 137-158.
5. Abdolhosseini Qomi, M.J., et al., *Combinatorial molecular optimization of cement hydrates*. Nat Commun, 2014. **5**.
6. Bhat, P.A. and N.C. Debnath, *Study of structures and properties of silica-based clusters and its application to modeling of nanostructures of cement paste by DFT methods*. IOP Conference Series: Materials Science and Engineering, 2013. **43**(1): p. 12001-12011.
7. R. Sánchez, M. Palacios, and F. Puertas, *Cementos petroleros con adición de escoria de horno alto. Características y propiedades*. Materiales de Construcción, 2011. **61**(302): p. 185-211.
8. Taddei, P., et al., *Vibrational study on the bioactivity of Portland cement-based materials for endodontic use*. Journal of Molecular Structure, 2009. **924–926**(0): p. 548-554.
9. Mendes, A., et al., *NMR, XRD, IR and synchrotron NEXAFS spectroscopic studies of OPC and OPC/slag cement paste hydrates*. Materials and Structures, 2011. **44**(10): p. 1773-1791.
10. Paluszkiwicz, C., et al., *Nucleation of hydroxyapatite layer on wollastonite material surface: FTIR studies*. Vibrational Spectroscopy, 2008. **48**(2): p. 263-268.
11. Radev, L., et al., *Organic/Inorganic bioactive materials Part II: in vitro bioactivity of Collagen-Calcium Phosphate Silicate/Wollastonite hybrids*. Central European Journal of Chemistry, 2009. **7**(4): p. 711-720.
12. Chukanov, N.V., *Infrared spectra of mineral species : extended library S. geochemistry/mineralogy*, Editor. 2014, Dordrecht : Springer, 2014.
13. Cong, X. and R.J. Kirkpatrick, *²⁹Si MAS NMR study of the structure of calcium silicate hydrate*. Advanced Cement Based Materials, 1996. **3**(3–4): p. 144-156.
14. Hansen, M.R., H.J. Jakobsen, and J. Skibsted, *²⁹Si Chemical Shift Anisotropies in Calcium Silicates from High-Field ²⁹Si MAS NMR Spectroscopy*. Inorganic Chemistry, 2003. **42**(7): p. 2368-2377.